Compressive Spectrum Sensing Based on Spectral Shape Feature Detection

Eva Lagunas and Montse Nájar
Department of Signal Theory and Communications
Universitat Politècnica de Catalunya (UPC), Barcelona, Spain
Email: {eva.lagunas,montse.najar}@upc.edu

***Abstract*—In this paper, we address sparsity-based spectrum sensing for Cognitive Radio (CR) applications. Motivated by the sparsity described by the low spectral occupancy of the licensed radios, the proposed approach utilizes the novel Compressive Sensing (CS) technique to alleviate the sampling burden in CR when processing very wide bandwidth. Instead of detecting underutilized subbands of the radio spectrum, this paper propose a feature-based strategy to detect the licensed holder activity from compressive measurements. The procedure follows the framework of correlation matching, changing the traditional single frequency scan to a spectral scan with the a priori known spectral shape of the licensed holder. In addition to the frequency-location estimate, the proposed technique is able to provide a power-level estimate and an estimation of the angle-of-arrival (AoA) of the primary users by circumventing the complex non-linear CS reconstruction.**

I. Introduction

The most critical design problem among the implementation challenges specific to spectrum sensing is the need to process a very wide bandwidth [1]. Moreover, with the current analog-to-digital converters (ADC) technology, wideband radio frequency signal digitising is a quite demanding task. Compressive Sensing (CS) is a recently proposed technique for data acquisition which offers the possibility of reducing the strong requirements of the ADCs based on the premise that the signal is sparse. The sparsity of the spectrum is often considered in the cognitive radio literature [2], [3] based on the low percentage of spectrum occupancy by active radios. In this paper, the sampling bottleneck is overcome using a particular CS technique called Multi-Coset (MC) sampling [4]. Unlike other sub-Nyquist sampling techniques, MC applies a periodic non-uniform sampling which preserves the structure needed for the computation of the compressed auto-correlation function. The correlation of compressive sampled data has also been considered in [5], [6] for finding underutilized bandwidth in crowded spectrum. Here, instead of detecting underutilized subbands of the radio spectrum, we propose a feature-based strategy to detect the licensed holder activity. The basic strategy is to compare the a priori known spectral shape of the primary user with the power spectral density of the received signal. Spectral feature detection with no data compression and no presence of interferent has been considered in [7]. Here, the comparison is made in a correlation matching framework since we do not have access to the power spectral density of the compressed signal. Furthermore, the correlation matching framework circumvents the non-linear l_1-minimization based CS reconstruction, which relies on a threshold or a regularization parameter that has to be appropriately optimized. Unlike [5], [6], this paper considers a multi-antenna receiver. The use of an antenna array allows us to obtain, besides a frequency-location and a power-level estimate, an estimation of the angle-of-arrival (AoA) of the primary users. The use of multi-antenna technologies is of great interest in CR since it allows to multiplex different users into the same channel at the same time in same geographical areas. Thus, the secondary nodes can use the AoA measurements to attain its transmission directivity and therefore increase the overall system capacity and reduce cochannel interference. This work extends previous authors' publications [8]–[10] to the case of compressive sensing and multiple receive antennas.

This paper is organized as follows. Section II states the signal model. Section III describes the compressive spectral detection scheme. Supporting results based on simulated data are provided in Section IV. Conclusions are drawn in Section V.

This work was partially supported by the Spanish Ministry of Science and Innovation (Ministerio de Ciencia e Innovación) under project TEC2011-29006-C03-02 (GRE3N-LINK-MAC), by the European Commission in the framework of the FP7 Network of Excellence in Wireless COMmunications NEWCOM# (Grant agreement no. 318306), by the Catalan Government under grant 2009 SGR 891 and by the European Cooperation in Science and Technology under project COST Action IC0902.

II. Compressed Signal Model

The basic idea of CR is spectral reusing or spectrum sharing, which allows the unlicensed users to communicate over licensed spectrum when the licensed holders are not fully utilizing it. Thus, we consider the received signal consists on the superposition of multiple primary and secondary (interference) services. The analytic representation of the received signal in a cognitive radio network can be expressed as,

$$r(t) = \sum_{k=1}^{K} a_k(t) e^{j(w_0+w_k)t} + n(t) \quad (1)$$

where $a_k(t)$ indicates the complex envelope of the source and w_k denotes the baseband frequency of the source with respect to the center frequency of the band under scrutiny w_0. A standard assumption in the literature is that $n(t)$ is AWGN.

Assuming a Nyquist-rate sampling T, each k-th source can be denoted by $\mathbf{b}_{k,m}$ meaning a m-th block of L-length Nyquist

ISBN 978-3-8007-3529-7

samples. To denote the m-th block of all the K sources present in the scenario we use $\mathbf{B}_m \in \mathbb{C}^{K\times L}$ defined as,

$$\mathbf{B}_m = \begin{bmatrix}\mathbf{b}_{1,m} & \cdots & \mathbf{b}_{k,m} & \cdots & \mathbf{b}_{K,m}\end{bmatrix}^T \quad (2)$$

The proposed spectrum sensing will be computed using multiple snapshots of measurements from a uniformly spaced linear array (ULA). According to (2), the complex snapshot of the received RF signal can be written as,

$$\mathbf{Z}_m = \mathbf{D}\mathbf{B}_m = \begin{bmatrix}\mathbf{z}_{1,m} & \cdots & \mathbf{z}_{n,m} & \cdots & \mathbf{z}_{N,m}\end{bmatrix}^T \quad (3)$$

where N is the number of antennas. Matrix $\mathbf{D} \in \mathbb{C}^{N\times K}$ is defined as,

$$\mathbf{D} = \begin{bmatrix}\mathbf{d}_1 & \cdots & \mathbf{d}_k & \cdots & \mathbf{d}_K\end{bmatrix} \quad (4)$$

where

$$\mathbf{d}_k = \begin{bmatrix}1 & e^{jw_0\frac{d}{c}\sin(\theta_k)} & \cdots & e^{jw_0(N-1)\frac{d}{c}\sin(\theta_k)}\end{bmatrix}^T \quad (5)$$

Here, d is the distance between two consecutive array elements, c is the speed of the light and θ_k is the angle of arrival of the k source. Note that (3) assumes the narrowband model, i.e, negligible group delay ($w_0 >> w_k$).

Throughout this paper, we will assume that the secondary users are independent of the noise and primary signal, and its spectral shape is different from that of the primary.

MC periodic non-uniform sampling is considered as acquisition technique. In MC sampling, we first pick a suitable sampling period. The inverse of this period will determine the base frequency of the system, being at least equal to the Nyquist rate so that sampling at ensures no aliasing. In general, this period is set equal to the Nyquist-period (T).

The MC sampling is applied at each antenna separately. Thus, towards the objective of fast data acquisition and assuming that wireless signals in open-spectrum networks are typically sparse in the frequency domain, consider the classical linear measurement model for each of the above antenna received signal,

$$\mathbf{y}_{n,m} = \Phi\mathbf{z}_{n,m} \quad (6)$$

Matrix Φ has dimension $p \times L$ and is known as compressive matrix. According to MC, Φ must be a matrix that randomly selects p samples of each $\mathbf{z}_{n,m}$, where $p < L$. This matrix Φ is given by randomly selecting p rows of the identity matrix $\mathbf{I}_L$. CS theory suggests that a low coherence between Φ and the basis where the signal becomes sparse (Fourier in our case) is desirable in order to ensure mutually independent matrices and therefore better compressive sampling [11]. In our example, the maximal incoherence associated to the Fourier basis is given by the canonical or spike basis, which is exactly the basis defined by the identity matrix.

The process of sampling described in (6) can be viewed as first sampling the signal at the Nyquist sampling rate (T) and then discarding all but p samples in every block of L samples periodically. Therefore, matrix Φ applies a non-uniform periodic sampling. Although MC sampling can be casted into a CS framework, its implementation becomes much more simpler: while usually CS considers an Analog to Information Converter (AIC), in the MC approach only a limited number of parallel ADCs operating at low sampling rate are needed [6].

Defining the compressive snapshot as,

$$\mathbf{Y}_m = \begin{bmatrix}\mathbf{y}_{1,m} & \cdots & \mathbf{y}_{n,m} & \cdots & \mathbf{y}_{N,m}\end{bmatrix}^T \quad (7)$$

the estimated data autocorrelation matrix can be obtained as follows,

$$\hat{\mathbf{R}}_y = \frac{1}{M}\sum_{m=1}^{M}\text{vec}(\mathbf{Y}_m)\text{vec}^H(\mathbf{Y}_m) \quad (8)$$

where $\text{vec}(\mathbf{Y}_m)$ is $\mathbb{C}^{pN\times 1}$ and denotes the concatenation of the p snapshots contained in $\mathbf{Y}_m$.

III. Compressive Spectral Featured Detection

The aim of this study is to approach the primary user detection problem from the feature-based detector perspective. More specifically, the traditional pure frequency line scanning is replaced by a scanning performed in terms of predefined spectral shape which corresponds to the spectral signature of the primary user that we aim to label. From the candidate spectral shape (that is how the baseband spectral shape of the licensed holder is labeled henceforth), the corresponding candidate autocorrelation matrix defined in base band ($\mathbf{R}_b$) can be easily obtained.

In order to explore the frequency dimension, the candidate base band autocorrelation matrix $\mathbf{R}_b$ is modulated by a rank-one matrix formed by the scanning frequency vector at the sensed frequency w as follows,

$$\mathbf{R}_c(w) = \left[\mathbf{R}_b \odot \mathbf{e}(w)\mathbf{e}^H(w)\right] \quad (9)$$

where $\odot$ denotes the elementwise product of two matrices, $\mathbf{e}(w) = \begin{bmatrix}1 & e^{jw} & \cdots & e^{j(L-1)w}\end{bmatrix}^T$. The resulting matrix has dimension $L \times L$.

The compressive version of (9) is given by,

$$\tilde{\mathbf{R}}_c(w) = \Phi\mathbf{R}_c(w)\Phi^T \quad (10)$$

An extended candidate correlation matrix must be built to cope with the angle of arrival dependency. The angle-dependent candidate correlation matrix can be obtained as follows,

$$\tilde{\mathbf{R}}_{cm}(w,\theta) = \mathbf{S}_\theta\tilde{\mathbf{R}}_c(w)\mathbf{S}_\theta^H \quad (11)$$

where matrix $\mathbf{S}_\theta$ is defined as $\mathbf{S}_\theta = \mathbf{I}_p \otimes \mathbf{s}_d^\theta$, with $\mathbf{I}_p$ being the identity matrix of dimension p, $\mathbf{s}_d^\theta = \begin{bmatrix}1 & e^{jw_0\frac{d}{c}\sin(\theta)} & \cdots & e^{jw_0(N-1)\frac{d}{c}\sin(\theta)}\end{bmatrix}^T$ and $\otimes$ denoting the Kronecker product. The dimensions of the general candidate correlation matrix are $\tilde{\mathbf{R}}_{cm}(w,\theta) \in \mathbb{C}^{pN\times pN}$.

According to this notation, the corresponding model for the data autocorrelation matrix defined in (8) is given by,

$$\begin{aligned}\tilde{\mathbf{R}}_y &= \sum_{i=1}^{N_x}\gamma(w_i)\mathbf{S}_{\theta_i}\Phi\left[\mathbf{R}_b \odot \mathbf{e}(w_i)\mathbf{e}^H(w_i)\right]\Phi^T\mathbf{S}_{\theta_i}^H + \tilde{\mathbf{R}}_n \\ &= \sum_{i=1}^{N_x}\gamma(w_i)\tilde{\mathbf{R}}_{cm}(w_i,\theta_i) + \tilde{\mathbf{R}}_n \end{aligned} \quad (12)$$

ISBN 978-3-8007-3529-7

where N_x indicates the number of primary sources present in the scenario, $\gamma(w_i)$ is the power level at the source frequency w_i and $\tilde{\mathbf{R}}_n$ is the compressed version of the noise plus interference.

Based on the previous assumptions, an estimate of the power level γ can be formulated as,

$$\min_{\gamma} \Psi\left(\hat{\mathbf{R}}_y, \gamma\tilde{\mathbf{R}}_{cm}(w,\theta)\right) \tag{13}$$

where $\Psi(\cdot,\cdot)$ is an error function between the two matrices. The suitable similarity function must work in low SNR scenarios, it must be robust to the presence of strong interference that secondary users may cause, and must operate with a low number of data records to guarantee short sensing time. Note that the solution to (13) will be clearly a function of the steering frequency and a function of the steering angle.

The different estimates result from the proper choice of the aforementioned error function. Three different error functions were discussed by the authors in [8]–[10]. The first one, which is based on the Euclidean distance, can be discarded due to the lack of interference rejection. In this work we focus on the other two methods: the one based on the geodesic distance and the one based on the positive semidefinite character of the autocorrelation matrices.

A. Spectrum Detector Based on the Geodesic Distance

The geodesic distance between $\hat{\mathbf{R}}_y$ and $\gamma\tilde{\mathbf{R}}_{cm}(w,\theta)$ is given by,

$$d^2_{geo}(\hat{\mathbf{R}}_y, \gamma\tilde{\mathbf{R}}_{cm}(w,\theta)) = \sum_{q=1}^{Q} \left(\ln(l_q)\right)^2 \tag{14}$$

where

$$\frac{1}{\gamma}(\tilde{\mathbf{R}}_{cm}(w,\theta))^{-1}\hat{\mathbf{R}}_y\mathbf{e}_q = l_q\mathbf{e}_q \quad \text{for} \quad q = 1,\ldots,Q \tag{15}$$

Minimizing (14) with respect to γ, we obtain the power level estimate (16a) and the resulting minimum geodesic distance (16b).

$$\gamma_G = \left(\prod_{q=1}^{Q}\lambda_q\right)^{\frac{1}{Q}} \tag{16a}$$

$$d^2_{geo,min} = \sum_{q=1}^{Q}\left|\ln\left(\lambda_q/\gamma_G\right)\right|^2 \tag{16b}$$

where λ_q $(q = 1,\ldots,Q)$ denotes the eigenvalues of $(\tilde{\mathbf{R}}_{cm}(w,\theta))^{-1}\hat{\mathbf{R}}_y$.

B. Spectrum Detector Based on the Minimum Eigenvalue

A second detector can be derived by forcing a positive semidefinite difference between the two matrices. The problem can be formulated as

$$\begin{aligned} \max_{\gamma\geq 0} \quad & \gamma \\ \text{s.t.} \quad & \hat{\mathbf{R}}_y - \gamma\tilde{\mathbf{R}}_{cm}(w,\theta) \succeq 0 \end{aligned} \tag{17}$$

TABLE I
SCENARIO CHARACTERISTICS

	Primary User	Interference
Modulation	BPSK	Pure Tone
Normalized Frequency(*)	0.2	0.3
AoA (degrees)	30	60
SNR (dB)	10	10

(*) The bandwidth under scrutiny is 10MHz.

If $\hat{\mathbf{R}}_y - \gamma\tilde{\mathbf{R}}_{cm}(w,\theta)$ must be positive semidefinite, $\mathbf{I} - \gamma\hat{\mathbf{R}}_y^{-1}\tilde{\mathbf{R}}_{cm}(w,\theta)$ must be too. Thus, using the EigenDecomposition of $\hat{\mathbf{R}}_y^{-1}\tilde{\mathbf{R}}_{cm}(w,\theta)$ defined by $\mathbf{U}\Lambda\mathbf{U}^H$,

$$\mathbf{I} - \gamma\mathbf{U}\Lambda\mathbf{U}^H \succeq 0 \;\Rightarrow\; \mathbf{I} - \gamma\Lambda \succeq 0 \;\Rightarrow\; \Lambda^{-1} - \gamma\mathbf{I} \succeq 0 \tag{18}$$

where Λ^{-1} is a diagonal matrix whose diagonal elements are the corresponding eigenvalues of the matrix $(\tilde{\mathbf{R}}_{cm}(w,\theta))^{-1}\hat{\mathbf{R}}_y$. In the worst case we assume that the minimum eigenvalue of $(\Lambda^{-1} - \gamma\mathbf{I})$ is equal to zero,

$$\lambda_{min}((\tilde{\mathbf{R}}_{cm}(w,\theta))^{-1}\hat{\mathbf{R}}_y) - \gamma = 0 \tag{19}$$

Thus, the solution to (17) is given by the minimum eigenvalue of $(\tilde{\mathbf{R}}_{cm}(w,\theta))^{-1}\hat{\mathbf{R}}_y$, that is,

$$\gamma_M = \lambda_{min}\left((\tilde{\mathbf{R}}_{cm}(w,\theta))^{-1}\hat{\mathbf{R}}_y\right) \tag{20}$$

IV. SIMULATION RESULTS

This section is divided in two parts. The first part concentrates on the general performance of the proposed method, where high SNR is used for the sake of figure clarity. The second part gives the ROC results for low SNR scenarios.

A. High SNR Scenario

To test the ability of the two proposed methods we first consider a scenario with a primary user with binary phase shift keying (BPSK) using rectangular pulse shape (4 samples per symbol) and a pure tone interference plus AWGN. The spectral occupancy (set of frequencies where the Fourier transform does not vanish) for this particular example is about 0.25. According to [12], the signal admits perfect reconstruction from periodic nonuniform sampling at rates approaching Landaus lower bound [13] equal to the measure of the spectral occupancy. Thus, if the spectral occupancy is 0.25, we can discard three of every fourth Nyquist samples. The array is composed of $N = 6$ antennas with an antenna separation equal to $\lambda/2$. The scenario characteristics have been summarized in Table I.

The size of the observed blocks is $L = 33$ samples. The sampling rates of $\mathbf{Y}_m$ and $\mathbf{Z}_m$ are related through the compression rate $\rho = \frac{p}{L}$. In order to force the size of the compressed observations to be the same for any compression rate (to ensure the quality of the autocorrelation matrix estimation), we set $M = 2L\epsilon\rho^{-1}$, where ϵ is a constant (in the following results $\epsilon = 30$). Thus, for a high compression rate, the estimator takes samples for a larger period of time.

ISBN 978-3-8007-3529-7

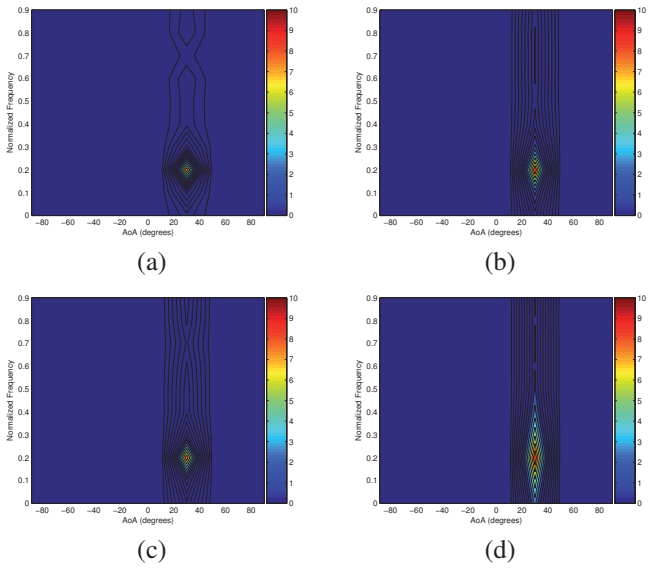

Fig. 1. Minimum Eigenvalue detector: γ_M for (a) ρ=1, (b) ρ=0.76, (c) ρ=0.52, (d) ρ=0.24.

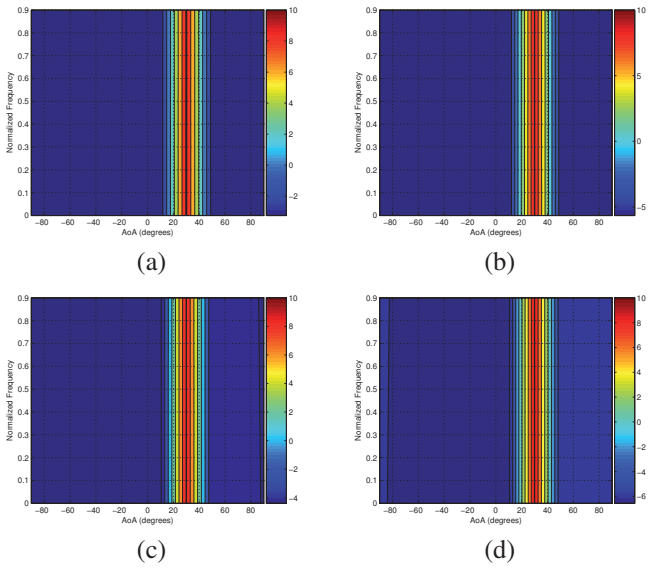

Fig. 3. Geodesic distance detector: power level γ_G for (a) ρ=1, (b) ρ=0.76, (c) ρ=0.52, (d) ρ=0.24.

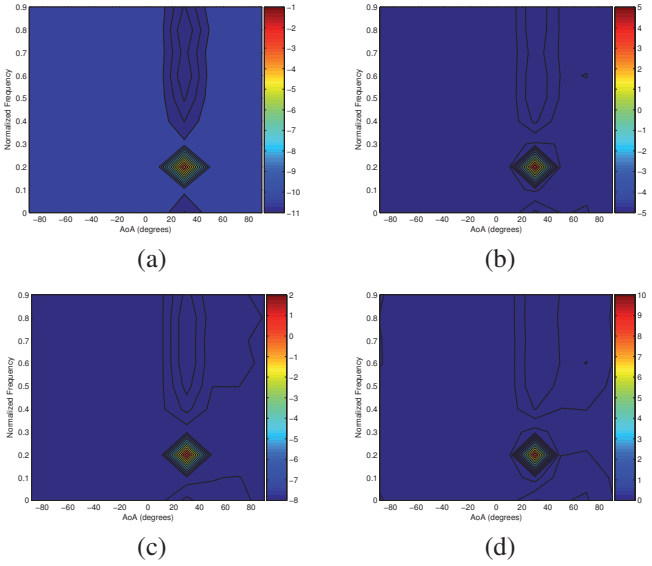

Fig. 2. Geodesic distance detector:: $d^{-1}_{geo,min}$ for (a) ρ=1, (b) ρ=0.76, (c) ρ=0.52, (d) ρ=0.24.

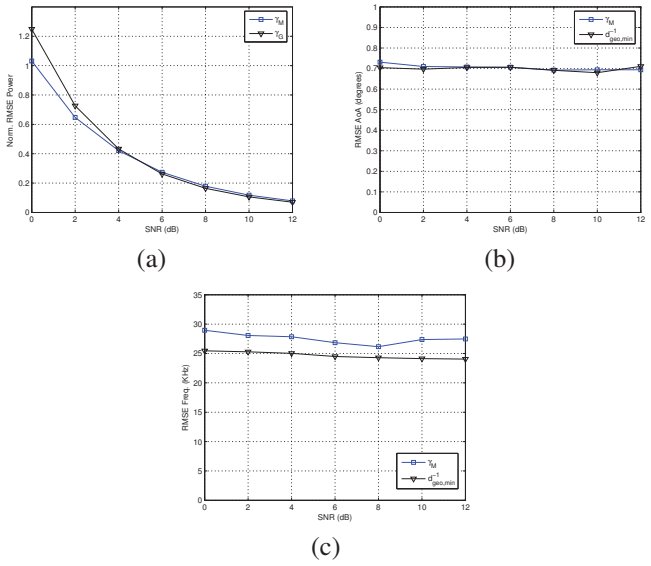

Fig. 4. RMSE for $\rho = 0.24$: (a) power level estimate, (b) AoA estimate and (c) frequency estimate.

Fig. 1 shows the performance of the Minimum Eigenvalue method (20) for different compression rates. The resulting estimate γ_M provides a clear estimate of the frequency and angle location, and produces a power level close to 10 dB, which coincides with the SNR. The interfering tone has disappeared due to the feature-based nature of the estimate. Although the compression affects the detection capabilities (the pick becomes wider in frequency axis), is interesting to note that the frequency, AoA and power level estimates do not suffer from the compression.

Fig. 2 and Fig. 3 shows the performance of the geodesic distance based detector. The independence of γ_G with respect to the carrier frequency could be observed in Fig. 3, where the value of γ_G only depends on the angle of arrival. The inverse of the geodesic distance is shown in Fig. 2. It shows higher robustness against the compression compared with γ_M, while providing an accurate estimation of the frequency and angle location.

Both methods achieve similar performance when multiple primary users are present, however, the results are not shown here for space reasons.

For the evaluation of the frequency, AoA and power estimation accuracy, an scenario with one active primary user with binary phase shift keying (BPSK) using a rectangular pulse

ISBN 978-3-8007-3529-7

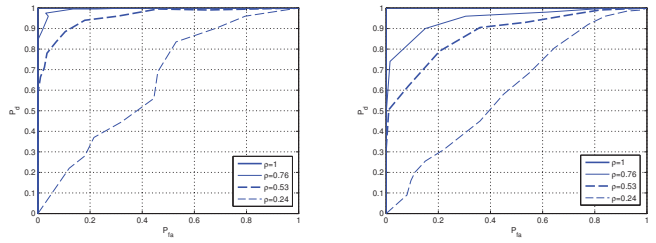

(a) (b)

Fig. 5. Geodesic distance detector ROC: (a) SNR=-14dB, (b) SNR=-16dB.

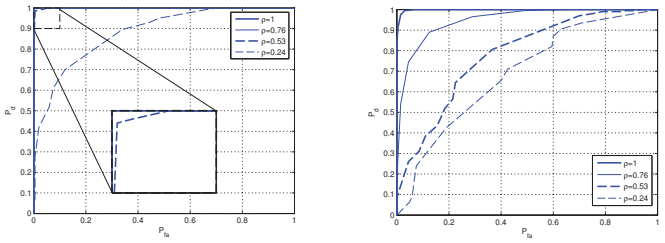

(a) (b)

Fig. 6. Minimum eigenvalue detector ROC: (a) SNR=-16dB, (b) SNR=-22dB.

shape (with 4 samples per symbol) and AWGN is considered. The frequency and angle location are chosen randomly in each of the 200 iterations. Here ϵ is equal to 10 and the grid resolution is 0.0078 and 1.4 degrees.

Fig. 4 show the normalized Root Mean Squared Error (RMSE) of the estimated power level (this is the RMSE divided by the SNR), the RMSE of the AoA estimation, and the RMSE of the estimated frequency location, respectively, using the Geodesic detector (blue) and the Minimum Eigenvalue detector (black) for $\rho = 0.24$. The results displayed in Fig. 4 show that the power level accuracy obtained with the Minimum eigenvalue detector is very similar to the one obtained with the Geodesic-based detector. Similarly, the AoA estimation accuracy remains almost constant for both detectors. However, is clear form Fig. 4(c) that γ_G provides better results than γ_M whatever the SNR used. This loss in frequency accuracy together with the preservation of the AoA accuracy agrees with the fact that the peak provided by γ_M becomes wider in the frequency axis as ρ decreases.

B. Low SNR Scenario

This section evaluates the performance in low SNR scenarios by means of the ROC curves. To evaluate the probability of false alarm versus the probability of detection we have run 200 simulations considering the presence of the primary user (Hypothesis H1), and 200 records of the same length without the primary user (Hypothesis H0). The primary user is located at w_s equal to 0.2 and angle of arrival equal to 30 degrees.

Again, the primary user is a BPSK (4 samples per symbol). No interference is considered here. Fig. 5(a) shows the ROC of $d^{-1}_{geo,min}$ for SNR=-14dB and Fig. 5(b) the ROC of $d^{-1}_{geo,min}$ for SNR=-16dB for different compression rates. As it was expected, the general performance of the Geodesic-based detector is deteriorated as the compression rate decreases.

Fig. 6 shows the ROCs for the Minimum Eigenvalue detector for (a) SNR=-16dB and (b) SNR=-22dB. The superiority of γ_M is clear from the comparison of Fig. 6 with Fig. 5, where the robustness of the γ_M is observed as the resulting plots for the geodesic-based detector are worse with respect to those obtained by the minimum eigenvalue detector.

V. Conclusion

A spectral feature detector for spectrum sensing based on periodic non-uniform sampling has been proposed in this paper. The basic strategy is to use the correlation matching with a predetermined spectral shape, which has to be known a priori. Two different techniques are studied: The first one, which is based on the geodesic distance, works well in terms of interference rejection and also provides good accuracy but the robustness against noise is quite poor. The second method, which is based on the positive semidefinite difference between matrices, provides the most compliant performance, offering acceptable accuracy of the estimated parameters and better robustness against noise.

References

[1] D. Cabric, S. M. Mishra, and R. W. Brodersen, "Implementation issues in Spectrum Sensing for Cognitive Radios," *Asilomar Conference on Signals, Systems and Computers*, vol. 1, pp. 772–776, Nov, 2004.

[2] Z. Tian and G. B. Giannakis, "Compressed Sensing for Wideband Cognitive Radios," *Inter. Conf. on Acoustics, Speech and Sig. Process. (ICASSP)*, pp. 1357–1360, May, 2008.

[3] M. Mishali and Y. Eldar, "From Theory to Practice: Sub-Nyquist Sampling of Sparse Wideband Analog Signals," *IEEE J. Sel. Topics Signal Processing*, vol. 4, no. 2, pp. 375–391, 2010.

[4] P. Feng, "Universal Minimum-Rate Sampling and Spectrum-Blind Reconstruction for Multiband Signals," *PhD, University of Illinois at Urbana-Champaign, USA*, 1997.

[5] D. Arianandа and G. Leus, "Compressive Wideband Power Spectrum Estimation," *IEEE Trans. Signal Process.*, pp. 4775–4788, Sep, 2012.

[6] M. A. Lexa, M. E. Davies, J. S. Thompson, and J. Nikolic, "Compressive Power Spectral Density Estimation," *Inter. Conf. on Acoustics, Speech and Sig. Process. (ICASSP)*, pp. 3884–3887, May, 2011.

[7] Z. Quan, W. Zhang, S. Shellhammer, and A. Sayed, "Optimal Spectral Feature Detection for Spectrum Sensing at Very Low SNR," *IEEE Trans. Commun.*, vol. 59, pp. 201–212, Jan, 2011.

[8] A. I. Pérez-Neira, M. A. Lagunas, M. A. Rojas, and P. Stoica, "Correlation Matching Approach for Spectrum Sensing in Open Spectrum Communications," *IEEE Trans. Sig. Process.*, vol. 57, no. 12, pp. 4823–4836, Dec, 2009.

[9] E. Lagunas and M. Najar, "Space-Time-Frequency Candidate Methods for Spectrum Sensing," *Europ. Sig. Process. Conf. (EUSIPCO)*, Aug, 2011.

[10] ——, "Space-Time-Frequency Candidate Methods for Spectrum Sensing," *EURASIP Journal on Adv. in Sig. Process., 2012:31*, Feb, 2012.

[11] E. J. Candes and M. B. Wakin, "An Introduction to Compressed Sampling," *IEEE Sig. Process. Magazine*, vol. 25, no. 2, pp. 21–30, Mar, 2008.

[12] R. Venkataramani and Y. Bresler, "Optimal Sub-Nyquist Nonuniform Sampling and Reconstruction for Multiband Signals," *IEEE Sig. Process. Letters*, vol. 18, no. 8, pp. 443–446, Aug, 2011.

[13] H. Landau, "Necessary density conditions for sampling and interpolation of certain entire functions," *Acta Math.*, vol. 117, no. 81, pp. 37–52, 1967.

ISBN 978-3-8007-3529-7